ANNUAL REVIEWS

*Annual Review of Microbiology*

# Compartmentalization of RNA Degradosomes in Bacteria Controls Accessibility to Substrates and Ensures Concerted Degradation of mRNA to Nucleotides

Agamemnon J. Carpousis,[1,2] Nathalie Campo,[1,*] Lydia Hadjeras,[1,3,*] and Lina Hamouche[1,*]

[1]LMGM, Université de Toulouse, CNRS, UPS, CBI, Toulouse, France; email: agamemnon.carpousis@univ-tlse3.fr, nathalie.campo@univ-tlse3.fr, lina_hamouche@hotmail.com

[2]TBI, Université de Toulouse, CNRS, INRAE, INSA, Toulouse, France

[3]Current affiliation: IMIB, University of Würzburg, Würzburg, Germany; email: lydia.hadjeras@uni-wuerzburg.de



Annu. Rev. Microbiol. 2022. 76:533–52

First published as a Review in Advance on June 7, 2022

The *Annual Review of Microbiology* is online at micro.annualreviews.org

https://doi.org/10.1146/annurev-micro-041020-113308



*These authors contributed equally to this article

## Keywords

BR-body, inner membrane protein, mRNA degradation, RNA degradosome, RNase E, ribosome assembly

## Abstract

RNA degradosomes are multienzyme complexes composed of ribonucleases, RNA helicases, and metabolic enzymes. RNase E–based degradosomes are widespread in *Proteobacteria*. The *Escherichia coli* RNA degradosome is sequestered from transcription in the nucleoid and translation in the cytoplasm by localization to the inner cytoplasmic membrane, where it forms short-lived clusters that are proposed to be sites of mRNA degradation. In *Caulobacter crescentus*, RNA degradosomes localize to ribonucleoprotein condensates in the interior of the cell [bacterial ribonucleoprotein-bodies (BR-bodies)], which have been proposed to drive the concerted degradation of mRNA to nucleotides. The turnover of mRNA in growing cells is important for maintaining pools of nucleotides for transcription and DNA replication.

Membrane attachment of the *E. coli* RNA degradosome is necessary to avoid wasteful degradation of intermediates in ribosome assembly. Sequestering RNA degradosomes to *C. crescentus* BR-bodies, which exclude structured RNA, could have a similar role in protecting intermediates in ribosome assembly from degradation.

## Contents



## 1. INTRODUCTION

RNA degradosomes are multienzyme mRNA-degrading complexes that exist under normal growth conditions and can be modified during stress (2, 9, 17, 58). In *Escherichia coli*, RNase E, which is the central component of the RNA degradosome, is an essential endoribonuclease that has a global role in the processing of stable RNA and the degradation of mRNA. The turnover of mRNA can be either constitutive or regulated. Constitutive mRNA turnover, which limits the lifetime of most mRNA to 2 or 3 min, is arguably the most important form of posttranscriptional regulation in *E. coli* because it permits a rapid reorganization of the transcriptome in response to transcriptional regulation. Regulated mRNA turnover involves RNA-binding proteins and regulatory RNAs that target specific classes of mRNA for degradation in which expression is silenced even though transcription of these mRNAs continues. For further reading about the mechanisms of mRNA degradation in *E. coli* and other bacteria, and the enzymes, proteins, and regulatory RNAs involved in these processes, we recommend the reviews in References 2, 9, 17, 18, 23, 58, 60, 72, 83, and 93.

Recent advances in imaging technology have transformed the field of bacterial cell biology. Previously considered to be noncompartmentalized, the bacterial cell is now appreciated to have complex higher-order organization. Despite the lack of organelles, bacteria can localize chromosome regions, plasmids, proteins, and RNA (34, 45, 68, 81, 87). Fluorescence microscopy with live cells showed that RNA degradosomes in *E. coli* are attached to the inner cytoplasmic membrane, where they form short-lived clusters that are proposed to be sites of mRNA degradation (31, 46, 84). In *Bacillus subtilis*, the endoribonuclease RNase Y also attaches to the inner cytoplasmic membrane, suggesting that compartmentalization of mRNA-degrading enzymes is generally important in bacteria. In *Caulobacter crescentus*, the RNA degradosome and mRNA are localized to bacterial ribonucleoprotein-bodies (BR-bodies), which are condensates formed by liquid-liquid phase separation (LLPS) (4, 5, 11, 67). Here, we review recent work showing that compartmentalization of the mRNA degradation machinery in *E. coli* and *C. crescentus* controls accessibility to RNA substrates and ensures concerted degradation of mRNA to nucleotides.

## 2. RNA DEGRADOSOMES IN BACTERIA AND PLANTS

RNase E of *E. coli* is the founding member of a large family of endoribonucleases that are widely distributed in bacteria and plants (2, 3). In *E. coli*, RNase E is a homotetrameric enzyme. The N-terminal half of each subunit folds into a compact globular structure that forms the catalytic domain, and the C-terminal noncatalytic region is predominantly natively unstructured protein (14, 15, 60). The noncatalytic region has small elements (15–40 amino acids) known as microdomains or short linear motifs that serve as sites of interaction with proteins, RNA, and phospholipid bilayers (2, 3, 60). The exoribonuclease PNPase, the glycolytic enzyme enolase, and the DEAD-box RNA helicase RhlB bind to microdomains to form a multienzyme complex known as the RNA degradosome (17). Another microdomain, known as the membrane targeting sequence (MTS), forms an amphipathic α-helix that binds to phospholipid bilayers (46, 84). Protein sequence comparisons have shown that RNase E homologs in the *Gammaproteobacteria* have a conserved N-terminal catalytic domain and a large natively unstructured C-terminal half with microdomains, including a conserved MTS (3). MTS-like microdomains have also been identified in RNase E homologs in *Betaproteobacteria* (46). These observations suggest that RNA degradosomes attached to the inner cytoplasmic membrane are found throughout the *Betaproteobacteria* and *Gammaproteobacteria*.

RNase E homologs, which have been identified in many different species of bacteria, have been classified into five types (2, 43, 49) (**Figure 1*a***). Each type of RNase E contains both the characteristic highly conserved catalytic domain and the noncatalytic C-terminal and/or N-terminal extensions, except the type IV enzymes. Type V enzymes are encoded in the plant nuclear genome and located in the chloroplast. In *Arabidopsis thaliana*, RNase E was found in the soluble fraction of a chloroplast extract (82). **Figure 1*b*** shows schematic diagrams of RNase E–based multienzyme complexes that have been characterized in various bacterial species. Proteins associated with RNase E vary depending on bacterial species (**Figure 1*b***). In general, RNase E interacts with exoribonucleases, RNA helicases, and metabolic enzymes (33, 39, 40, 49, 94). Some RNase E homologs, for example, from *Streptomyces coelicolor* and *Pseudoalteromonas haloplanktis*, can replace *E. coli* RNase E (1, 49). In the case of *P. haloplanktis*, which is a gammaproteobacterium distantly related to *E. coli*, the RNase E–RhlB interaction is conserved, whereas the RNase E–PNPase interaction is species specific (3). The variability in RNA degradosome composition is due to plasticity in the sequence of the natively unstructured C-terminal half of RNase E, which is free from constraints on structure that are normally associated with compact globular proteins. Thus, although the sequence of the N-terminal catalytic domain is highly conserved, the sequence of the C-terminal half of RNase E diverges even in closely related bacterial species (3). The rapid evolution of the microdomains results in species-specific protein interactions.

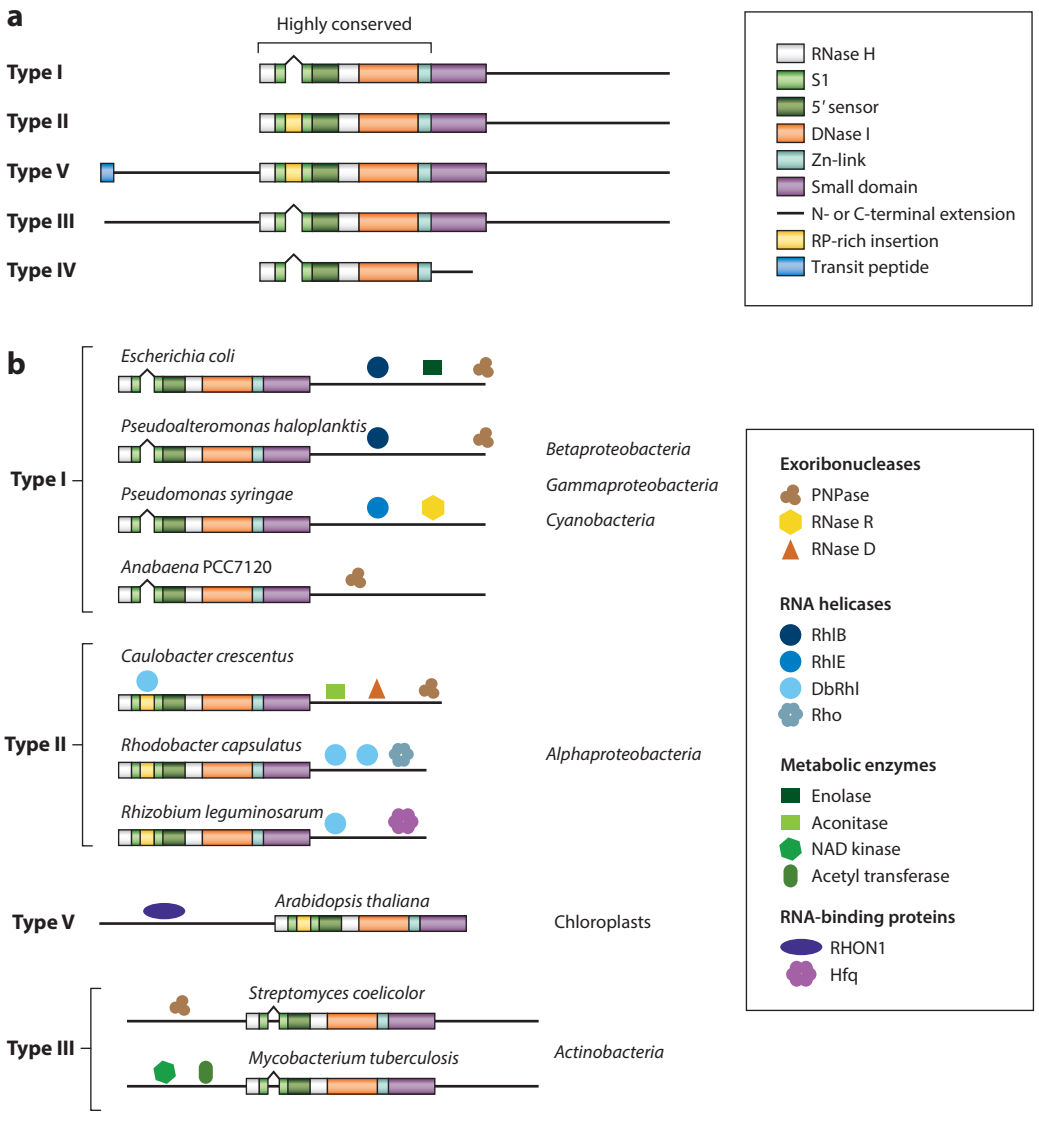


**Figure 1**

RNase E homologs and RNA degradosomes. (*a*) RNase E homologs can be classified into five types on the basis of protein sequence comparisons. The color-coded legend shows conserved protein folds in the catalytic domain: RNase H, S1 RNA-binding domain, 5′ sensor, DNase I, and Zn-link, as well as noncatalytic N- and C-terminal extensions. The small domain is a conserved structural element except in the type IV enzymes. The arginine-proline (RP)-rich region is an element inserted into the S1 domain in the type II and V enzymes. The transit peptide is a conserved element at the N-terminal end of type V enzymes. (*b*) Composition of RNA degradosomes from diverse species of bacteria and plants. The schematic diagrams show RNase E and the approximate position of the site of binding of the associated proteins. The color-coded legend shows the associated proteins sorted into four classes on the basis of activity: exoribonucleases, RNA helicases, metabolic enzymes, and RNA-binding proteins. Adapted from Reference 2.

For the purpose of this review, note that RNase E homologs in the *Betaproteobacteria* and *Gammaproteobacteria* are type I enzymes with large C-terminal regions containing multiple microdomains, including an MTS. RNase E homologs in the *Alphaproteobacteria* are distinguished from the type I enzymes by the insertion of the arginine-proline (RP)-rich element into the

catalytic domain and the lack of an identifiable MTS. In *C. crescentus*, RNase E has been localized to the interior of the cell (56).

## 3. COMPARTMENTALIZATION OF TRANSCRIPTION AND TRANSLATION IN THE BACTERIAL CELL

### 3.1. The Super-Resolution Revolution

As the cellular localization and dynamics of proteins and nucleic acids are an important part of the work reviewed here, we briefly describe recent advances in fluorescence microscopy, which is a powerful tool with which to study the internal architecture of the bacterial cell. The development of fluorescent proteins (FPs) and synthetic fluorophores combined with various fluorescence microscope setups has revolutionized our ability to study the localization and dynamics of proteins in bacteria (80). Bacteria are small objects with dimensions on the order of micrometers. Classical light microscopy is diffraction limited, meaning that it is not possible to resolve two objects that are separated by less than half the wavelength of visible light (200–300 nm) (35, 77). Although wide-field microscopy is diffraction limited, it is still possible to obtain useful information about the localization of bacterial proteins tagged with FPs. The development of epifluorescence microscopy for use in bacterial molecular genetics was driven in part by work on cell growth and division. Proteins involved in these processes are often localized to sites that are associated with machineries for DNA replication, chromosome partition, and cell division (96). The methodologies described below were developed in part to overcome the limits of classical light microscopy.

Total internal reflection fluorescence microscopy (TIRFm) is a powerful technique that greatly increases contrast and therefore sensitivity (6, 98). In TIRFm, an evanescence wave that is approximately 100 nm deep illuminates FPs closest to the side of the cell that abuts the coverslip. This configuration is ideal for imaging proteins localized to the membrane. It is possible to adjust a TIRF microscope to a highly inclined and laminated optical (HILO), or a dirty TIRF configuration, that illuminates a thin sheet of cells (90). Owing to their excellent signal-to-noise ratio, TIRFm and HILOm are particularly suitable for single-molecule tracking (SMT) and quantitative analyses of dynamic movements (98).

Another advance has been the development of photo-switchable fluorescent probes (pFPs), which are proteins or synthetic dyes that blink, whereas FPs continually emit light (54, 95). Because a molecule that blinks can be treated as a point source, pFP-tagged proteins can be localized with a spatial resolution of approximately 30 nm, which is tenfold better than diffraction-limited microscopy. Single-molecule super-resolution images are made with photoactivated localization microscopy (PALM) or stochastic optical reconstruction microscopy (STORM) setups, which operate using the same principles (12, 76). pFP-tagged proteins are illuminated using low-intensity excitation light, resulting in the blinking of thousands of molecules over several minutes. At the same time, the emitted light is captured by a high-speed video. The image is then reconstructed using positions recorded in the video. An important advance is the use of optical astigmatism combined with STORM imaging (3D-STORM), which permits localization in all three dimensions (36). With the development of appropriate computing methods, it is now possible to reconstruct 3D images from a field of cells, thus permitting statistical analyses of protein localization and distribution (51, 55).

There is a large choice of FPs and pFPs available, as well as synthetic fluorescent ligands that can be covalently attached to a protein known as the Halo Tag (54). Issues that need to be considered when working with FPs for live-cell imaging in bacteria include rates of maturation, intrinsic brightness, sensitivity to photobleaching, and the potential for aggregation (24, 95). The photocenters of FPs are formed by a maturation process involving the spontaneous oxidation of amino

acid residues, which can take up to 60 min (80). Because rapidly growing bacterial cells often have a doubling time shorter than the maturation time, a large proportion of the FPs are immature molecules that do not fluoresce. The intrinsic brightness of an FP and resistance to photobleaching are also important factors that affect the limits of detection. Some FPs promote aggregation, which in turn can affect activity and localization (16). For this reason, FP-tagged proteins should be expressed using single-copy constructs under endogenous expression signals to avoid overexpression, which can contribute to aggregation. Many FPs have been modified to decrease their tendency to aggregate (95). The resulting derivatives, which are often labeled as monomeric FPs (e.g., mCherry, mVenus, mMaple3), are proteins of choice for imaging live bacterial cells.

The techniques described in this section have revolutionized our ability to localize and track proteins in live bacterial cells. It is now possible to analyze hundreds or thousands of cells under conditions that maintain cell integrity and viability. It is also feasible to measure changes in localization and dynamics when live cells are subjected to stresses such as treatment with antibiotics and starvation for nutrients.

## 3.2. Exclusion of Ribosomes from the Nucleoid

In the period before the discovery that DNA is the hereditary material, bacteriologists worked mainly in hospitals and identified pathogenic bacteria using growth on various nutrient media, colony size and morphology, and microscopy of fixed and stained cells. While bacterial cells were seen to have characteristic sizes and shapes (99), their interior was perceived as transparent, with no visible structure. With the discovery that DNA is the hereditary material, researchers became interested in defining the size, composition, and localization of bacterial chromosomes. We direct the interested reader to the authoritative review by Robinow & Kellenberger (74) on research during the second half of the twentieth century, involving mainly *E. coli* and *B. subtilis*, that led to the identification and characterization of the bacterial nucleoid. In consideration of this historical work, the nucleoid, which is the site of transcription, was defined as a membraneless structure containing DNA, RNA, and protein. The cytoplasm, which is densely packed with ribosomes and thus the site of translation, was defined as the region between the nucleoid and the plasma membrane.

Recent work investigating nucleoid size and cell size in a large number of bacteria and under different growth conditions showed that the nucleoid size–to–cell size ratio (NC ratio) is a conserved characteristic of a bacterial species that does not correlate with chromosome size or growth rate (28) (**Figure 2*a*,*b***). There is, however, a negative correlation between cell size and NC ratio. That is, species with smaller cells tend to have larger NC ratios. Of particular interest for this review are the model bacterial organisms *E. coli*, *B. subtilis*, and *C. crescentus*, which represent three deeply separated phyla of bacteria: *Gammaproteobacteria*, *Firmicutes*, and *Alphaproteobacteria*, respectively. *E. coli* and *B. subtilis* are large bacteria with clearly defined nucleoids and similar NC ratios of approximately 0.40. In contrast, *C. crescentus* and related *Alphaproteobacteria* have smaller cells with NC ratios in the range of 0.70 to 0.90.

The NC ratio correlates with ribosome dynamics and organization of translation (28) (**Figure 2*c***). Ribosome diffusion was measured by SMT with FP-labeled ribosomal proteins (r-proteins). Distribution of ribosomes was measured by fluorescence in situ hybridization (FISH) via a probe specific to a conserved sequence in the 3′ end of 16S rRNA. Exclusion of ribosomes from the nucleoids of *E. coli* and *B. subtilis* (low NC ratios) is consistent with the historical definition of the bacterial nucleoid and cytoplasm (7, 53, 74). Although these results do not exclude the possibility of low levels of coupled transcription–translation in the nucleoid of bacteria with low NC ratios, recent experimental work strongly suggests that uncoupled transcription–translation is predominant in *B. subtilis* and many other bacteria (42). Furthermore, a recent review raises

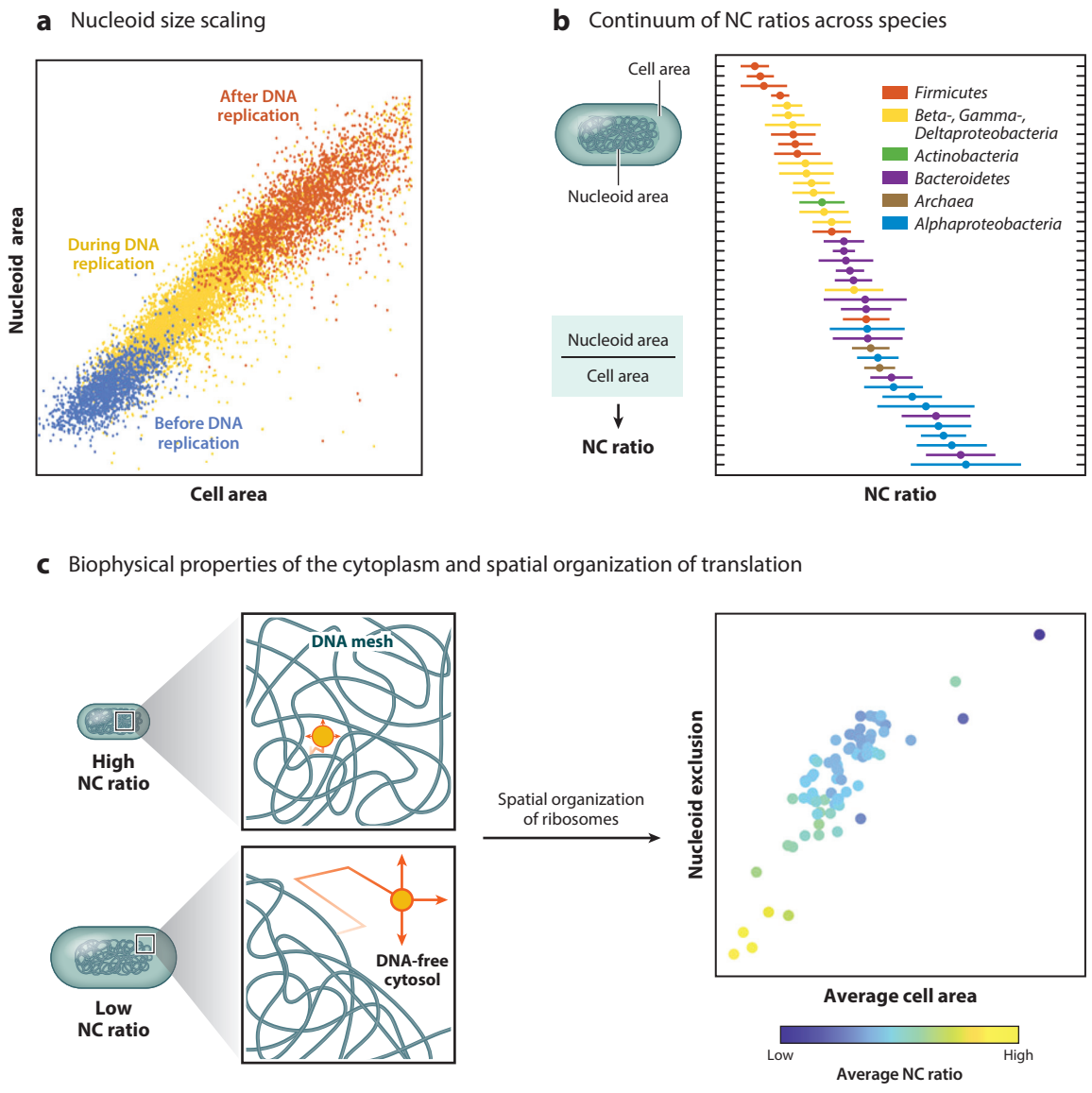


**Figure 2**

Nucleoid size–to–cell size ratio (NC ratio) and exclusion of ribosomes from the nucleoid. (*a*) Nucleoid size scaling. During cell growth and DNA replication, the NC ratio is constant. Each point corresponds to the measurement of the image of a single cell. Colors refer to stages of growth as indicated. Area refers to the size measured in the analysis of 2D images. (*b*) NC ratios vary across species. NC ratios are a characteristic property of a bacterial species. Species are color coded by phyla. The dot shows the average NC value; the horizontal line shows the standard deviation. (*c*) Biophysical properties of the cytoplasm and spatial organization of translation. Ribosomes are excluded from the nucleoid in species with low NC ratios, whereas they colocalize with the nucleoid in species with high NC ratios. Ribosome diffusion in the nucleoid is constrained by the DNA meshwork of the highly compacted chromosome. The graph shows the relationship between exclusion of ribosomes from the nucleoid and NC ratios for individual species (*dots*). Colors correspond to a heat map showing a range of NC ratios. Adapted with permission from Reference 28.

the possibility that coupled transcription–translation in *E. coli* is limited to a few specialized transcription units (38). In contrast to the internal architecture of *E. coli* and *B. subtilis*, there is no separation of nucleoid and cytoplasm in *C. crescentus* (28). The historical definition of the bacterial nucleoid and cytoplasm therefore needs to be generalized in consideration of experimental work showing that there is a range of internal architectures in which the separation of transcription and translation depends on the NC ratio (**Figure 2*c***). As described below, differences in the compartmentalization of transcription and translation have important functional consequences on how ribosome assembly and mRNA degradation are organized in the bacterial cell.

### 3.3. The *E. coli* RNA Degradosome

As evidenced by epifluorescence and TIRFm, RNase E forms short-lived clusters on the inner cytoplasmic membrane (31, 84). We prefer the term puncta to distinguish small point-like clusters from larger clusters, which we term foci. RhlB and PNPase display the same localization and dynamics as RNase E (31). Colocalization analyses demonstrated that these components of the RNA degradosome track with RNase E. RNA degradosome puncta appear to move on the inner cytoplasmic membrane, but this movement could be an illusion owing to the rapid formation and dissociation of clusters over a few seconds. Inhibition of transcription by rifampicin depletes mRNA and precursors of rRNA and tRNA and disassembles RNA degradosome puncta, suggesting that RNA substrate is required for clustering. However, this proposition has been revised since recent work has shown that kasugamycin, which inhibits the initiation of translation, also disassembles RNA degradosome puncta (31). Although there is low-level translation of leaderless mRNA in the presence of kasugamycin, velocity sedimentation analyses showed that polyribosomes are not formed (44, 64). Because transcription continues in the presence of kasugamycin, the formation of RNA degradosome puncta was therefore proposed to result from an interaction with polyribosomes. Taken together, these experimental results suggest that puncta are sites of mRNA degradation in which the initial step involves the capture of polyribosomes by the RNA degradosome. The disappearance of puncta could involve the dissociation of RNA degradosomes from polyribosomes or the disassembly of polyribosomes as mRNA is degraded.

**Figure 3** shows a model for polyribosome-mediated clustering of the RNA degradosome on the inner membrane of *E. coli*. Biochemical work has shown that the RNA degradosome binds ribosomes and polyribosomes, thus supporting a direct interaction (91) (**Figure 3*a***). After rifampicin treatment, polyribosomes are disassembled and RNA degradosome puncta disappear (**Figure 3*b***). After kasugamycin treatment, formation of polyribosomes is inhibited, which also results in the disappearance of RNA degradosome puncta (**Figure 3*c***). Because transcription continues in the presence of kasugamycin, the degradation of ribosome-free mRNA does not promote formation of RNA degradosome puncta. This model has implications for the cell biology of mRNA decay in *E. coli*. Scanning of polyribosomes could be either passive or active. Passive scanning would involve a random search for regions of ribosome-free mRNA in the polyribosome, whereas active scanning would involve direct competition between the binding of ribosomes and RNA degradosomes to the translation initiation region at the 5′ end of the mRNA. These modes of initiation of mRNA degradation are not necessarily mutually exclusive. Furthermore, posttranscriptional regulation, for instance, by RNA-binding proteins or regulatory RNAs that inhibit translation, is expected to produce ribosome-free mRNA that bypasses the scanning of polyribosomes and directly interacts with the RNA degradosome. This mode of degradation could be rapid because in the cell, diffusion of ribosome-free mRNA is expected to be much faster than diffusion of ribosomes or polyribosomes (28). The depletion of mRNA that is targeted for degradation by regulatory molecules in cells where synthesis of the mRNA continues is consistent

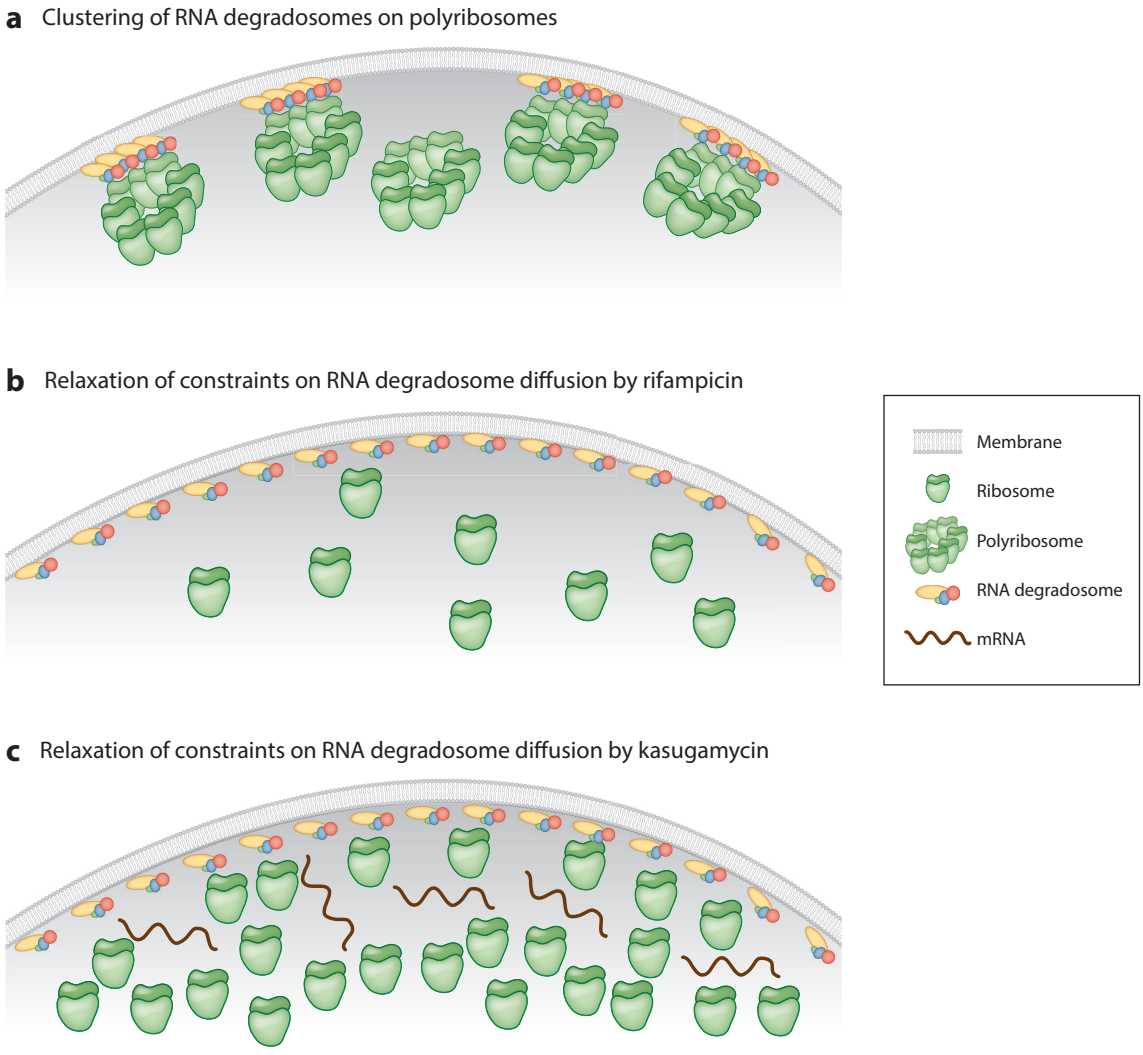


**Figure 3**

Model of clustering of RNA degradosomes by polyribosomes. (*a*) Clustering of RNA degradosomes on polyribosomes. Multiple RNA degradosomes associate transiently with polyribosomes to scan for exposed regions of mRNA that can be cleaved by RNase E to initiate degradation. (*b*) Relaxation of constraints on RNA degradosome diffusion by rifampicin. Disruption of polyribosomes after depletion of mRNA by rifampicin treatment results in randomly distributed RNA degradosomes. (*c*) Relaxation of constraints on RNA degradosome diffusion by kasugamycin. Disruption of polyribosomes after inhibition of translation initiation by kasugamycin treatment results in randomly distributed RNA degradosomes. Adapted from Reference 31.

with a rapid ribosome-free mode of mRNA degradation (83, 93). These considerations suggest significant differences between the mechanism of degradation of polyribosomal mRNA and ribosome-free mRNA due to the compartmentalization of the mRNA degradation machinery.

Recent work suggests that the RNA degradosome can be displaced from the inner cytoplasmic membrane under conditions of stress. Upon transition from aerobic to anaerobic growth, cells become filamentous and RNase E localizes to the interior of the cell in a diffuse pattern (66). Starving *E. coli* of a nitrogen source causes a single large focus of RNase E to form (61). Treatment

of cells with the protein synthesis inhibitor chloramphenicol results in foci of RNase E that are not attached to the inner cytoplasmic membrane (31). These results suggest that stress-induced detachment of RNase E from the inner membrane could control RNase E activity or accessibility to RNA substrates.

### 3.4. Binding to the Inner Membrane Does Not Modulate the Catalytic Activity of RNase E

Although RNase E is an essential enzyme in *E. coli*, mutant strains encoding variants in which part or all of the C-terminal region is deleted are viable (52, 57, 70, 92). Binding to the inner cytoplasmic membrane of *E. coli* is disrupted in mutant strains in which the amphipathic α-helix encoded by the RNase E MTS is mutated by amino acid substitution or deletion (46). In the *rneΔMTS* background, cytoplasmic RNase E (cRNase E) uniformly localizes to the interior of the cell (46, 63, 84). The *rneΔMTS* strain exhibits a slow-growth phenotype, a slowdown of mRNA degradation, and disruption of RNA quality control (29). Although a previous study proposed that membrane localization of RNase E preferentially destabilizes mRNA encoding inner membrane proteins (63), this preference was not considered statistically significant in a subsequent study (29) that determined the slowdown in mRNA degradation is global. Control experiments showed that the level of cRNase E in the *rneΔMTS* strain is the same as the level of membrane-attached RNase E in the $rne^+$ strain. These results raise the question of whether binding to the inner membrane boosts the catalytic activity of RNase E.

Enzyme assays employing RNase E and 9S rRNA as substrate showed that neither phospholipid vesicles nor nonionic detergent, which is necessary to solubilize the wild-type enzyme, affected endoribonuclease activity (46). These results suggest that binding to phospholipid bilayers or detergent does not modulate the catalytic activity of RNase E. A Michaelis–Menten analysis showed that deletion of the MTS had no effect on $k_{cat}$, whereas there was a small 40% increase in $K_m$, which could involve the incorporation of the wild-type enzyme into detergent micelles (29). This result suggests that the MTS, which is separated from the catalytic domain by approximately 50 residues, does not functionally interact with the catalytic domain to regulate activity (29). Nevertheless, it has been proposed that electrostatic interactions with the phospholipid bilayer stabilize the catalytic core of RNase E and facilitate the binding of RNA substrate (65). This proposal is consistent with the observation that cRNase E is unstable (29). On balance, the experimental evidence suggests that attachment of RNase E to the phospholipid bilayer does not directly affect catalytic activity, although the environment of the inner cytoplasmic membrane could affect enzyme stability and substrate affinity.

### 3.5. The *Helicobacter pylori* RNA Degradosome

After the discovery of the RNA degradosome in *E. coli*, multienzyme assemblies similar to the RNA degradosome have been identified in diverse bacterial species. These assemblies, which are sometimes based on ribonucleases different from RNase E, have also been termed degradosomes. In *Helicobacter pylori*, posttranscriptional regulation and adaptation to gastric colonization rely largely on a multienzyme complex composed of the essential ribonuclease RNase J, which has both exo- and endoribonuclease activity, and the DEAD-box RNA helicase RhpA (25, 73). This multienzyme complex therefore has activities analogous to those of the *E. coli* RNA degradosome, but the enzymes in the *H. pylori* RNA degradosome are not homologs of the *E. coli* enzymes. RNase J and RhpA are localized to the inner membrane in the form of foci as evidenced by cell fractionation experiments and super-resolution microscopy (88). Focus formation is mediated by RNA substrate and the bacterial membrane scaffolding protein flotillin (89). It was thus proposed

that foci are hubs of mRNA degradation. This work shows that *Helicobacter*, which is an epsilonproteobacterium, has membrane-attached mRNA-degrading machinery like the *Betaproteobacteria* and *Gammaproteobacteria*, reinforcing the notion that compartmentalization of this machinery can be achieved by localization to the inner membrane.

### 3.6. mRNA Degradation in Gram-Positive Bacteria

The principal endoribonuclease initiating mRNA decay in *B. subtilis*, RNase Y, has cleavage specificity similar to that of *E. coli* RNase E as well as a global impact on mRNA stability (78). Because RNase Y and RNase E have no sequence or structural homology, these ribonucleases appear to have arisen by convergent evolution. RNase Y is attached to the inner membrane by a short N-terminal transmembrane domain (19, 37). An RNase Y homolog in the pathogen *Staphylococcus aureus* is also a membrane-attached endoribonuclease (47). The use of TIRFm and SMT showed that *B. subtilis* RNase Y diffused rapidly on the membrane in the form of short-lived puncta, which increase in size and number when transcription is arrested by rifampicin. Puncta formation thus appears to be independent of RNA substrate availability (30). Three small proteins forming the Y-complex (YaaT, YlbF, and YmcA) were shown to interact functionally with RNase Y and to have a role in the maturation of polycistronic mRNA (22). The Y-complex has been proposed to modulate RNase Y activity by shifting the distribution of RNase Y to smaller and fewer complexes (30). These results reveal significant differences between RNase E– and RNase Y–based degradation machineries. Further work is needed to clarify the role of RNase Y puncta in the processing and degradation of mRNA.

On the basis of mapping protein–protein interactions by two-hybrid analysis, it was proposed that RNase Y in *B. subtilis* organized a degradosome-like complex composed of enolase, phosphofructokinase, the RNA helicase CshA, PNPase, and RNase J1/J2 (20, 50). A similar putative complex in *S. aureus* was described (72, 75). However, unlike the RNase E–based degradosome in *E. coli*, the *B. subtilis* degradosome remains enigmatic because chemical cross-linking is required to capture interactions. Furthermore, recent localization by fluorescence microscopy has shown that most of the predicted components of the *B. subtilis* RNA degradosome are cytoplasmic, which contrasts with the membrane localization of RNase Y (19). On balance, the experimental evidence strongly suggests that interactions with RNase Y are transient and thus not indicative of a stable multienzyme complex.

## 4. CELLULAR LOCALIZATION OF RNA DEGRADOSOMES CONTROLS ACCESS TO RNA SUBSTRATES

### 4.1. Transcription, Translation, and mRNA Degradation in *E. coli*

*E. coli* has a compact nucleoid that occupies approximately 40% of the cell (28) (**Figure 2**). RNA polymerase in live cells is localized to the nucleoid as evidenced by super-resolution imaging, whereas the surrounding cytoplasm is densely packed with ribosomes, thus confirming the separation of transcription and translation (7). Rifampicin treatment showed that RNA polymerase forms dense clusters in fast-growing *E. coli* cells and that clustering is structured in the nucleoid independent of RNA synthesis (97). SMT measurements revealed two types of RNA polymerase clusters: actively transcribing and nontranscribing (48). The confinement of nontranscribing RNA polymerase to clusters could help accelerate the reinitiation of rRNA synthesis, which is a major activity in growing cells. Additional work showed that hexanediol treatment led to the disappearance of RNA polymerase clusters. This result suggests that clustering is due to LLPS, which is a common phenomenon involving the formation of membraneless compartments that sequester

molecules and organize enzymatic reactions (8). LLPS formation occurs when proteins and nucleic acids form multiple transient and multivalent interactions, resulting in the formation of a liquid-like condensate that is physically separated from other macromolecules.

Super-resolution imaging of live *E. coli* cells has shown that greater than 85% of RNase E is localized to the inner cytoplasmic membrane (63). Low density along the central axis of the cell shows that RNase E is absent from the nucleoid. This work has contributed significantly to the view that mRNA degradation in *E. coli* is tightly membrane associated and thus separated from transcription in the nucleoid.

## 4.2. Ribosome Biogenesis in *E. coli*

Over the past two decades, evidence has emerged that rRNA processing and ribosome assembly are organized spatially (13). In *E. coli*, most rRNA operons are in close proximity in the nucleoid, leading to the suggestion that there is a bacterial nucleolus (27). rRNA operons are transcribed as a single precursor, 30S rRNA, which then undergoes extensive processing carried out by a battery of ribonucleases, including RNase III and RNase E (23, 41, 79, 86). Some of these maturation steps take place on nascent rRNA in the nucleoid (**Figure 4*a***). Evidence for cotranscriptional processing of rRNA comes from electron microscopy (EM) studies known as Miller spreads (62). Cleavage of nascent rRNA by RNase III gives a characteristic double-arrow morphology, with the shorter transcript corresponding to 16S rRNA and the longer transcript corresponding to 23S rRNA, thus providing direct evidence that the initial processing of rRNA by RNase III is cotranscriptional. RNA FISH showed that the 5′ leader sequence of 30S rRNA is localized to the nucleoid, that the 17S precursor of 16S rRNA is localized to the cytoplasm, and that this separation is RNase III dependent (59). These results show that early steps in ribosome biogenesis occur cotranscriptionally in the nucleoid but that late steps in rRNA processing, for example, by RNase E, occur after intermediates in ribosome assembly are released from the nucleoid.

Ribosome biogenesis is a complex multistep process that requires the coordinated synthesis of rRNA and r-proteins (21, 79). rRNA folding is driven by the binding of r-proteins and occurs in distinct structural units (blocks) (**Figure 4*b*,*c***). That is, subunits are assembled via multiple parallel pathways, each of which produces rate-limiting intermediates and unproductive side paths (21, 79). In addition to r-protein binding and rRNA folding, a large number of assembly factors, including enzymes, modify rRNA, RNA helicases and protein chaperons. Errors in biogenesis result in defective ribosomal subunits that could interfere with translation. Recent work has shown that rRNA in defective ribosomal subunits is eliminated by degradation of translationally inactive particles, which is initiated by RNase E cleavage (10, 32, 85, 100). This work leads to the proposal that the membrane-attached RNA degradosome scans newly synthesized ribosomal subunits as part of a quality-control mechanism in which correctly assembled particles are matured by trimming 5′ and 3′ extensions of the 17S and 9S rRNA precursors to 16S and 5S rRNA, respectively, whereas defective particles are degraded on the inner cytoplasmic membrane by the RNA degradosome (**Figure 4*d***).

## 4.3. Degradation of Intermediates in Ribosome Assembly by Cytoplasmic RNase E

Recent work with the *E. coli rneΔMTS* strain expressing cRNase E revealed an abnormal ribosome profile with high levels of 20S and 40S particles (L. Hadjeras, M. Bouvier, I. Canal, Q. Morin-Ogier, L. Poljak, et al., manuscript in preparation). 5′- and 3′-end analysis of their RNA showed that the 20S and 40S particles contained precursors of 16S rRNA and of 23S and 5S rRNA, respectively. Analysis of their protein content showed that they were deficient in a subset

of ribosomal proteins and that they contained assembly factors that are not detected in mature 30S and 50S ribosomal subunits. RNA in the 20S and 40S particles also contained 3′ untemplated oligo(A) tracks, suggesting that they are intermediates in degradation. Mapping endoribonuclease cleavages in rRNA from the subparticles revealed sites whose sequence corresponds to the

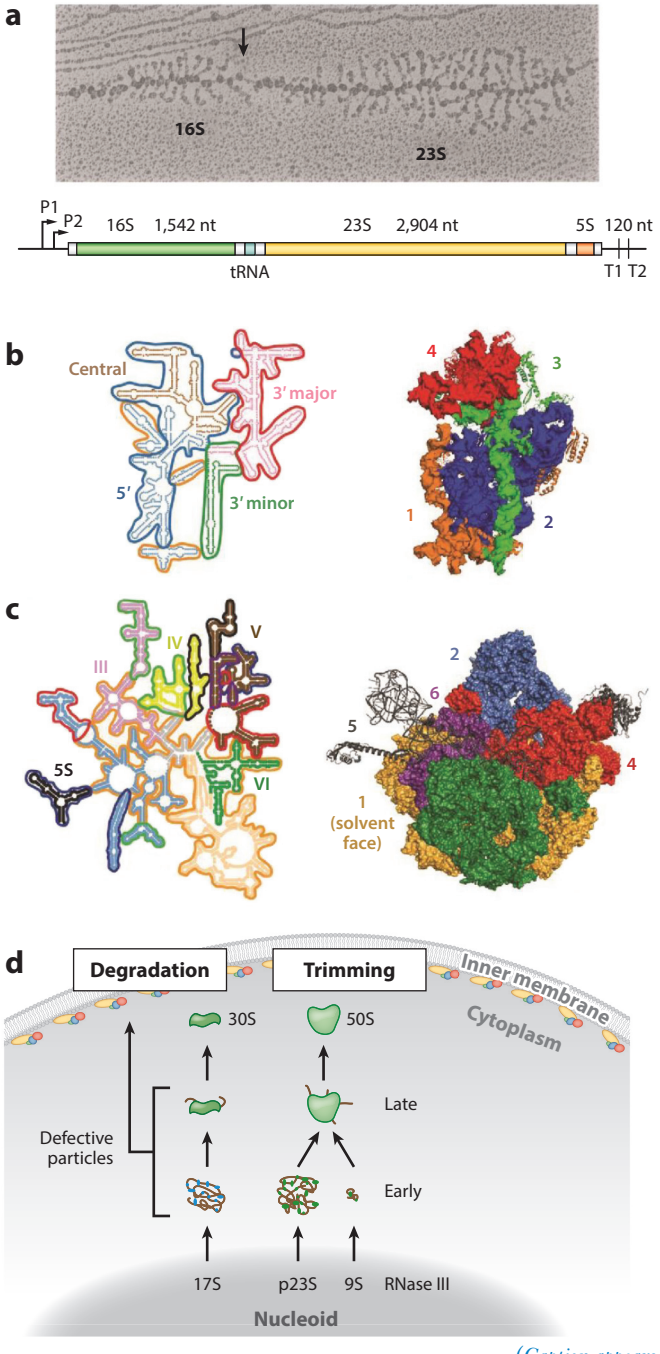


(Caption appears on following page)

**Figure 4** (*Figure appears on preceding page*)

Cellular organization of ribosome biogenesis in *Escherichia coli*. (*a*) Electron microscopy image of a Miller spread aligned with a map of an rRNA operon. The arrow indicates a point where the 16S precursor is released from the chromosome by RNase III cleavage. The dense blobs on the DNA are RNA polymerase. The dense blobs on nascent rRNA are ribosomal proteins that bind cotranscriptionally. (*b*,*c*) Folding blocks in 16S and 23S rRNA. Schematic diagram of rRNA secondary structure with folding blocks (*left*) and structural model of ribosomal subunits with domains corresponding to folding blocks (*right*). Color coding indicates the correspondence between folding blocks and domains in the structural model. (*d*) Schematic diagram showing release of early intermediates in ribosome assembly from the nucleoid, maturation in the cytoplasm, and trimming on the inner cytoplasmic membrane of precursor rRNA in mature particles. An alternate pathway is shown in which defective intermediates in ribosome assembly are degraded on the inner cytoplasmic membrane by the RNA degradosome. The inner membrane and RNA degradosome are drawn as in **Figure 3**. Panels *a–c* are adapted from Reference 21.

consensus for RNase E cleavage. In vitro experiments with purified RNase E and ribosomes showed that properly folded ribosomes are resistant to RNase E cleavage, whereas rRNA in ribosomes that were partially unfolded are cleaved by RNase E at the same sites that were mapped in vivo. Analysis of mutant strains in which the activities of poly(A)polymerase, PNPase, and RNase R were deficient showed that these enzymes are involved in the exonucleolytic degradation of rRNA fragments. This work shows that cRNase E nicks intermediates in ribosome assembly before they have a chance to fold into mature particles, resulting in the degradation of rRNA.

Nicking of rRNA by cRNase E is a stochastic process in which maturation of a ribosomal subunit and rRNA degradation compete. Ribosome biogenesis is a major activity in growing cells. The time it takes for a cell to double is directly related to the time it takes to double ribosome content. Because rRNA synthesis is the rate-limiting step in ribosome biogenesis (71), the wasteful degradation of rRNA likely explains the slower rate of growth of the *rneΔMTS* strain compared with the *rne*$^{+}$ strain (29, 46). Recent work has shown the importance of competition between RNase E substrates in setting rates of mRNA degradation (26, 69). Furthermore, enzymes involved in rRNA and mRNA degradation are the same (10, 18, 32, 85, 100). Because a major proportion of transcription in growing cells is rRNA synthesis, competition between rRNA and mRNA degradation could explain the global slowdown in mRNA degradation in the *rneΔMTS* strain (29). This work shows that membrane attachment of RNase E as a component of the RNA degradosome is necessary to avoid a futile cycle of degradation of intermediates in ribosome assembly. Conservation of membrane-associated RNase E throughout the *Betaproteobacteria* and *Gammaproteobacteria* could be due to selective pressure to avoid interference with ribosome biogenesis.

## 4.4. *Caulobacter crescentus* mRNA Degradation in Ribonucleoprotein Condensates

The RNA degradosome of *C. crescentus* is localized to the interior of the cell in condensates known as bacterial ribonucleoprotein-bodies (BR-bodies), which have properties similar to eukaryotic stress granules and processing bodies (4, 11). These RNA–protein condensates are formed by LLPS as evidenced by their sensitivity to hexanediol treatment in vivo and their reconstitution in vitro with purified components. Rifampicin treatment has demonstrated that assembly of BR-bodies is dynamic and requires RNA substrate. The endoribonuclease activity of RNase E is necessary for disassembly of BR-bodies. The intrinsically unstructured C-terminal domain (CTD) of RNase E, which is conserved in the *Alphaproteobacteria*, is necessary and sufficient for the formation of condensates with RNA as evidenced in vivo by the disruption of BR-bodies when the CTD is deleted and the formation of BR-bodies when the CTD is expressed by itself. It was thus proposed that the *C. crescentus* BR-body is a compartment nucleated by the RNA degradosome in which mRNA is degraded.

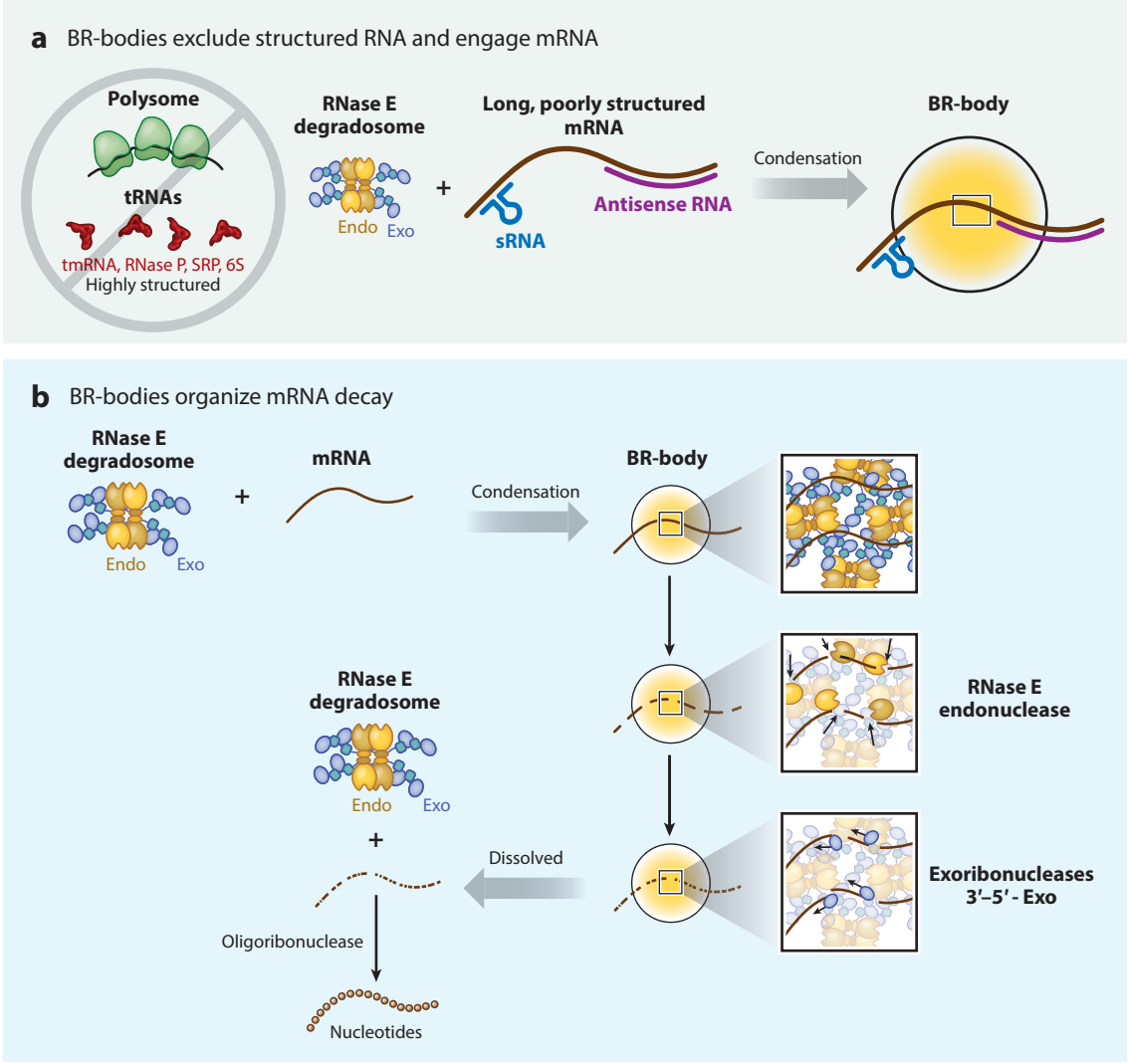


**Figure 5**

*Caulobacter crescentus* BR-bodies are sites of mRNA degradation. (*a*) BR-bodies are formed by interactions with single-stranded mRNA. Ribosome and highly structured RNA are excluded from BR-bodies. The model suggests that ribosome-free mRNA is required to initiate BR-body formation. (*b*) BR-bodies organize mRNA decay. Pathway in which mRNA is degraded to nucleotides in a concerted process that involves BR-body formation, endonucleolytic cleavage by RNase E, and exonucleolytic cleavage by 3′–5′ exoribonucleases, resulting in concerted degradation to nucleotides. Adapted with permission from Reference 5. Abbreviations: BR-body, bacterial ribonucleoprotein-body; sRNA, soluble RNA; tmRNA, transfer-messenger RNA.

Characterization of the RNA content of *C. crescentus* BR-bodies showed that they are enriched in mRNAs and that rRNA and tRNA are excluded (5) (**Figure 5*a***). Selective permeability of the BR-body enriches mRNA and mRNA decay intermediates, thus increasing their concentration and driving degradation to nucleotides, which is important for maintaining nucleotide pools for transcription and DNA replication in growing cells. Because polyribosomes are excluded from BR-bodies, it was proposed that there is a competition between initiation of translation by

ribosomes and inhibition of translation by binding of the RNA degradosome to the translation initiation region of mRNA (**Figure 5*b***). Ribosome-free mRNA associated with the RNA degradosome then condenses into BR-bodies, where it is degraded. Importantly, BR-bodies form a compartment that is distinct from the nucleoid and cytoplasm. These results suggest that intermediates in ribosome assembly in *C. crescentus* are protected from nicking by cytoplasmic RNase E owing to the sequestration of the RNA degradosome into condensates that exclude structured RNA.

## 5. CONCLUSION

mRNA degradation in *E. coli* and *C. crescentus* is physically separated from transcription and translation in membraneless compartments. These bacteria, which are separated by billions of years of evolution, use different strategies to achieve similar outcomes. Short-lived RNA degradosome puncta on the inner cytoplasmic membrane of *E. coli* are centers of mRNA degradation. The membrane-attached RNA degradosome is also involved in processing of rRNA and quality control of ribosomes. The physical separation of the RNA degradosome on the inner membrane from early steps in ribosome biogenesis in the nucleoid is necessary to prevent degradation of intermediates in ribosome assembly. The compartmentalization of RNA degradosomes in *C. crescentus* BR-bodies has functions similar to the membrane attachment of *E. coli* RNase E. BR-bodies are condensates in which the RNA degradosome and ribosome-free mRNA are concentrated, thus driving degradation to nucleotides. BR-bodies exclude ribosomes and polyribosomes, thus segregating translation from mRNA degradation. BR-body formation could also be involved in protecting intermediates in ribosome assembly from wasteful degradation. Compartmentalization of the mRNA-degrading machinery in *E. coli* and *C. crescentus* is a fascinating example of convergent evolution in which different cellular architectures result in different solutions to similar problems involving the accessibility of RNA substrates to the RNA degradosome and the concerted degradation of mRNA to nucleotides.

## DISCLOSURE STATEMENT

The authors are not aware of any affiliations, memberships, funding or financial holdings that could be perceived as a conflict of interest.

## ACKNOWLEDGMENTS

Research in Toulouse has been supported by grants to A.J.C. from the Agence Nationale de la Recherche (memRNase, ANR-13-BSV6-0005; IB-mRND, ANR-16-CE12-0014). We thank Muriel Cocaign-Bousquet, Ben Luisi, and Peter Redder for helpful suggestions to improve this review.

## LITERATURE CITED

1. Aït-Bara S, Carpousis AJ. 2010. Characterization of the RNA degradosome of *Pseudoalteromonas haloplanktis*: conservation of the RNase E-RhlB interaction in the Gammaproteobacteria. *J. Bacteriol.* 192:5413–23
2. Aït-Bara S, Carpousis AJ. 2015. RNA degradosomes in bacteria and chloroplasts: classification, distribution and evolution of RNase E homologs. *Mol. Microbiol.* 97:1021–35
3. Aït-Bara S, Carpousis AJ, Quentin Y. 2015. RNase E in the γ-Proteobacteria: conservation of intrinsically disordered noncatalytic region and molecular evolution of microdomains. *Mol. Genet. Genom.* 290:847–62
4. Al-Husini N, Tomares DT, Bitar O, Childers WS, Schrader JM. 2018. α-Proteobacterial RNA degradosomes assemble liquid-liquid phase-separated RNP bodies. *Mol. Cell* 71:1027–39.e14

5. Al-Husini N, Tomares DT, Pfaffenberger ZJ, Muthunayake NS, Samad MA, et al. 2020. BR-bodies provide selectively permeable condensates that stimulate mRNA decay and prevent release of decay intermediates. *Mol. Cell* 78:670–82.e8
6. Axelrod D, Burghardt TP, Thompson NL. 1984. Total internal reflection fluorescence. *Annu. Rev. Biophys. Bioeng.* 13:247–68
7. Bakshi S, Siryaporn A, Goulian M, Weisshaar JC. 2012. Superresolution imaging of ribosomes and RNA polymerase in live *Escherichia coli* cells. *Mol. Microbiol.* 85:21–38
8. Banani SF, Lee HO, Hyman AA, Rosen MK. 2017. Biomolecular condensates: organizers of cellular biochemistry. *Nat. Rev. Mol. Cell Biol.* 18:285–98
9. Bandyra KJ, Bouvier M, Carpousis AJ, Luisi BF. 2013. The social fabric of the RNA degradosome. *Biochim. Biophys. Acta Gene Regul. Mech.* 1829:514–22
10. Basturea GN, Zundel MA, Deutscher MP. 2011. Degradation of ribosomal RNA during starvation: comparison to quality control during steady-state growth and a role for RNase PH. *RNA* 17:338–45
11. Bayas CA, Wang J, Lee MK, Schrader JM, Shapiro L, Moerner WE. 2018. Spatial organization and dynamics of RNase E and ribosomes in *Caulobacter crescentus*. *PNAS* 115:E3712–21
12. Betzig E, Patterson GH, Sougrat R, Lindwasser OW, Olenych S, et al. 2006. Imaging intracellular fluorescent proteins at nanometer resolution. *Science* 313:1642–45
13. Bohne A-V. 2014. The nucleoid as a site of rRNA processing and ribosome assembly. *Front. Plant Sci.* 5:257
14. Callaghan AJ, Aurikko JP, Ilag LL, Gunter Grossmann J, Chandran V, et al. 2004. Studies of the RNA degradosome-organizing domain of the *Escherichia coli* ribonuclease RNase E. *J. Mol. Biol.* 340:965–79
15. Callaghan AJ, Marcaida MJ, Stead JA, McDowall KJ, Scott WG, Luisi BF. 2005. Structure of *Escherichia coli* RNase E catalytic domain and implications for RNA turnover. *Nature* 437:1187–91
16. Cambrée A, Aertsen A. 2020. Bacterial vivisection: how fluorescence-based imaging techniques shed a light on the inner workings of bacteria. *Microbiol. Mol. Biol. Rev.* 84(4):e00008-20
17. Carpousis AJ. 2007. The RNA degradosome of *Escherichia coli*: an mRNA-degrading machine assembled on RNase E. *Annu. Rev. Microbiol.* 61:71–87
18. Carpousis AJ, Luisi BF, McDowall KJ. 2009. Endonucleolytic initiation of mRNA decay in *Escherichia coli*. *Prog. Mol. Biol. Transl. Sci.* 85:91–135
19. Cascante-Estepa N, Gunka K, Stülke J. 2016. Localization of components of the RNA-degrading machine in *Bacillus subtilis*. *Front. Microbiol.* 7:1492
20. Commichau FM, Rothe FM, Herzberg C, Wagner E, Hellwig D, et al. 2009. Novel activities of glycolytic enzymes in *Bacillus subtilis*: interactions with essential proteins involved in mRNA processing. *Mol. Cell Proteom.* 8:1350–60
21. Davis JH, Williamson JR. 2017. Structure and dynamics of bacterial ribosome biogenesis. *Philos. Trans. R. Soc. B* 372(1716):20160181
22. DeLoughery A, Lalanne JB, Losick R, Li GW. 2018. Maturation of polycistronic mRNAs by the endoribonuclease RNase Y and its associated Y-complex in *Bacillus subtilis*. *PNAS* 115:E5585–94
23. Deutscher MP. 2009. Maturation and degradation of ribosomal RNA in bacteria. *Prog. Mol. Biol. Transl. Sci.* 85:369–91
24. Durisic N, Laparra-Cuervo L, Sandoval-Alvarez Á, Borbely JS, Lakadamyali M. 2014. Single-molecule evaluation of fluorescent protein photoactivation efficiency using an in vivo nanotemplate. *Nat. Methods* 11:156–62
25. El Mortaji L, Aubert S, Galtier E, Schmitt C, Anger K, et al. 2018. The sole DEAD-box RNA helicase of the gastric pathogen *Helicobacter pylori* is essential for colonization. *mBio* 9(2):e02071-17
26. Etienne TA, Cocaign-Bousquet M, Ropers D. 2020. Competitive effects in bacterial mRNA decay. *J. Theor. Biol.* 504:110333
27. Gaal T, Bratton BP, Sanchez-Vazquez P, Sliwicki A, Sliwicki K, et al. 2016. Colocalization of distant chromosomal loci in space in *E. coli*: a bacterial nucleolus. *Genes Dev.* 30:2272–85
28. Gray WT, Govers SK, Xiang Y, Parry BR, Campos M, et al. 2019. Nucleoid size scaling and intracellular organization of translation across bacteria. *Cell* 177:1632–48.e20

29. Hadjeras L, Poljak L, Bouvier M, Morin-Ogier Q, Canal I, et al. 2019. Detachment of the RNA degradosome from the inner membrane of *Escherichia coli* results in a global slowdown of mRNA degradation, proteolysis of RNase E and increased turnover of ribosome-free transcripts. *Mol. Microbiol.* 111:1715–31
30. Hamouche L, Billaudeau C, Rocca A, Chastanet A, Ngo S, et al. 2020. Dynamic membrane localization of RNase Y in *Bacillus subtilis*. *mBio* 11(1):e03337-19
31. Hamouche L, Poljak L, Carpousis AJ. 2021. Polyribosome-dependent clustering of membrane-anchored RNA degradosomes to form sites of mRNA degradation in *Escherichia coli*. *mBio* 12(5):e0193221
32. Hamouche L, Poljak L, Carpousis AJ. 2021. Ribosomal RNA degradation induced by the bacterial RNA polymerase inhibitor rifampicin. *RNA* 27(8):946–58
33. Hardwick SW, Chan VS, Broadhurst RW, Luisi BF. 2011. An RNA degradosome assembly in *Caulobacter crescentus*. *Nucleic Acids Res.* 39:1449–59
34. Hiraga S. 2000. Dynamic localization of bacterial and plasmid chromosomes. *Annu. Rev. Genet.* 34:21–59
35. Huang B, Babcock H, Zhuang X. 2010. Breaking the diffraction barrier: super-resolution imaging of cells. *Cell* 143:1047–58
36. Huang B, Wang W, Bates M, Zhuang X. 2008. Three-dimensional super-resolution imaging by stochastic optical reconstruction microscopy. *Science* 319:810–13
37. Hunt A, Rawlins JP, Thomaides HB, Errington J. 2006. Functional analysis of 11 putative essential genes in *Bacillus subtilis*. *Microbiology* 152:2895–907
38. Irastortza-Olaziregi M, Amster-Choder O. 2020. Coupled transcription-translation in prokaryotes: an old couple with new surprises. *Front. Microbiol.* 11:624830
39. Jager S, Fuhrmann O, Heck C, Hebermehl M, Schiltz E, et al. 2001. An mRNA degrading complex in *Rhodobacter capsulatus*. *Nucleic Acids Res.* 29:4581–88
40. Jager S, Hebermehl M, Schiltz E, Klug G. 2004. Composition and activity of the *Rhodobacter capsulatus* degradosome vary under different oxygen concentrations. *J. Mol. Microbiol. Biotechnol.* 7:148–54
41. Jain C. 2020. RNase AM, a 5′ to 3′ exonuclease, matures the 5′ end of all three ribosomal RNAs in *E. coli*. *Nucleic Acids Res.* 48:5616–23
42. Johnson GE, Lalanne JB, Peters ML, Li GW. 2020. Functionally uncoupled transcription-translation in *Bacillus subtilis*. *Nature* 585:124–28
43. Kaberdin VR, Miczak A, Jakobsen JS, Lin-Chao S, McDowall KJ, von Gabain A. 1998. The endoribonucleolytic N-terminal half of *Escherichia coli* RNase E is evolutionarily conserved in *Synechocystis* sp. and other bacteria but not the C-terminal half, which is sufficient for degradosome assembly. *PNAS* 95:11637–42
44. Kaberdina AC, Szaflarski W, Nierhaus KH, Moll I. 2009. An unexpected type of ribosomes induced by kasugamycin: a look into ancestral times of protein synthesis? *Mol. Cell* 33:227–36
45. Keiler KC. 2011. RNA localization in bacteria. *Curr. Opin. Microbiol.* 14:155–59
46. Khemici V, Poljak L, Luisi BF, Carpousis AJ. 2008. The RNase E of *Escherichia coli* is a membrane-binding protein. *Mol. Microbiol.* 70:799–813
47. Khemici V, Prados J, Linder P, Redder P. 2015. Decay-initiating endoribonucleolytic cleavage by RNase Y is kept under tight control via sequence preference and sub-cellular localisation. *PLOS Genet.* 11:e1005577
48. Ladouceur AM, Parmar BS, Biedzinski S, Wall J, Tope SG, et al. 2020. Clusters of bacterial RNA polymerase are biomolecular condensates that assemble through liquid-liquid phase separation. *PNAS* 117:18540–49
49. Lee K, Cohen SN. 2003. A *Streptomyces coelicolor* functional orthologue of *Escherichia coli* RNase E shows shuffling of catalytic and PNPase-binding domains. *Mol. Microbiol.* 48:349–60
50. Lehnik-Habrink M, Newman J, Rothe FM, Solovyova AS, Rodrigues C, et al. 2011. RNase Y in *Bacillus subtilis*: a natively disordered protein that is the functional equivalent of RNase E from *Escherichia coli*. *J. Bacteriol.* 193:5431–41
51. Lelek M, Gyparaki MT, Beliu G, Schueder F, Griffié J, et al. 2021. Single-molecule localization microscopy. *Nat. Rev. Methods Primers* 1:39
52. Leroy A, Vanzo NF, Sousa S, Dreyfus M, Carpousis AJ. 2002. Function in *Escherichia coli* of the non-catalytic part of RNase E: role in the degradation of ribosome-free mRNA. *Mol. Microbiol.* 45:1231–43

53. Lewis PJ, Thaker SD, Errington J. 2000. Compartmentalization of transcription and translation in *Bacillus subtilis*. *EMBO J.* 19:710–18
54. Li H, Vaughan JC. 2018. Switchable fluorophores for single-molecule localization microscopy. *Chem. Rev.* 118:9412–54
55. Liu Z, Lavis LD, Betzig E. 2015. Imaging live-cell dynamics and structure at the single-molecule level. *Mol. Cell* 58:644–59
56. Llopis PM, Jackson AF, Sliusarenko O, Surovtsev I, Heinritz J, et al. 2010. Spatial organization of the flow of genetic information in bacteria. *Nature* 466:77–81
57. Lopez PJ, Marchand I, Joyce SA, Dreyfus M. 1999. The C-terminal half of RNase E, which organizes the *Escherichia coli* degradosome, participates in mRNA degradation but not rRNA processing in vivo. *Mol. Microbiol.* 33:188–99
58. Mackie GA. 2013. RNase E: at the interface of bacterial RNA processing and decay. *Nat. Rev. Microbiol.* 11:45–57
59. Malagon F. 2013. RNase III is required for localization to the nucleoid of the 5′ pre-rRNA leader and for optimal induction of rRNA synthesis in *E. coli*. *RNA* 19:1200–7
60. Marcaida MJ, DePristo MA, Chandran V, Carpousis AJ, Luisi BF. 2006. The RNA degradosome: life in the fast lane of adaptive molecular evolution. *Trends Biochem. Sci.* 31:359–65
61. McQuail J, Carpousis AJ, Wigneshweraraj S. 2022. The association between Hfq and RNase E in long-term nitrogen-starved *Escherichia coli*. *Mol. Microbiol.* 117(1):54–66
62. Miller OL Jr., Hamkalo BA, Thomas CA Jr. 1970. Visualization of bacterial genes in action. *Science* 169:392–95
63. Moffitt JR, Pandey S, Boettiger AN, Wang S, Zhuang X. 2016. Spatial organization shapes the turnover of a bacterial transcriptome. *eLife* 5:e13065
64. Müller C, Sokol L, Vesper O, Sauert M, Moll I. 2016. Insights into the stress response triggered by kasugamycin in *Escherichia coli*. *Antibiotics* 5(2):19
65. Murashko ON, Kaberdin VR, Lin-Chao S. 2012. Membrane binding of *Escherichia coli* RNase E catalytic domain stabilizes protein structure and increases RNA substrate affinity. *PNAS* 109:7019–24
66. Murashko ON, Lin-Chao S. 2017. *Escherichia coli* responds to environmental changes using enolasic degradosomes and stabilized DicF sRNA to alter cellular morphology. *PNAS* 114:E8025–34
67. Muthunayake NS, Tomares DT, Childers WS, Schrader JM. 2020. Phase-separated bacterial ribonucleoprotein bodies organize mRNA decay. *Wiley Interdiscip. Rev. RNA* 11:e1599
68. Nevo-Dinur K, Govindarajan S, Amster-Choder O. 2012. Subcellular localization of RNA and proteins in prokaryotes. *Trends Genet.* 28:314–22
69. Nouaille S, Mondeil S, Finoux AL, Moulis C, Girbal L, Cocaign-Bousquet M. 2017. The stability of an mRNA is influenced by its concentration: a potential physical mechanism to regulate gene expression. *Nucleic Acids Res.* 45:11711–24
70. Ow MC, Liu Q, Kushner SR. 2000. Analysis of mRNA decay and rRNA processing in *Escherichia coli* in the absence of RNase E-based degradosome assembly. *Mol. Microbiol.* 38:854–66
71. Paul BJ, Ross W, Gaal T, Gourse RL. 2004. rRNA transcription in *Escherichia coli*. *Annu. Rev. Genet.* 38:749–70
72. Redder P. 2018. Molecular and genetic interactions of the RNA degradation machineries in Firmicute bacteria. *Wiley Interdiscip. Rev. RNA* 9:e1460
73. Redko Y, Aubert S, Stachowicz A, Lenormand P, Namane A, et al. 2013. A minimal bacterial RNase J-based degradosome is associated with translating ribosomes. *Nucleic Acids Res.* 41:288–301
74. Robinow C, Kellenberger E. 1994. The bacterial nucleoid revisited. *Microbiol. Rev.* 58:211–32
75. Roux CM, DeMuth JP, Dunman PM. 2011. Characterization of components of the *Staphylococcus aureus* mRNA degradosome holoenzyme-like complex. *J. Bacteriol.* 193:5520–26
76. Rust MJ, Bates M, Zhuang X. 2006. Sub-diffraction-limit imaging by stochastic optical reconstruction microscopy (STORM). *Nat. Methods* 3:793–95
77. Schermelleh L, Heintzmann R, Leonhardt H. 2010. A guide to super-resolution fluorescence microscopy. *J. Cell Biol.* 190:165–75
78. Shahbabian K, Jamalli A, Zig L, Putzer H. 2009. RNase Y, a novel endoribonuclease, initiates riboswitch turnover in *Bacillus subtilis*. *EMBO J.* 28:2523–33

79. Shajani Z, Sykes MT, Williamson JR. 2011. Assembly of bacterial ribosomes. *Annu. Rev. Biochem.* 80:501–26
80. Shaner NC, Steinbach PA, Tsien RY. 2005. A guide to choosing fluorescent proteins. *Nat. Methods* 2:905–9
81. Shapiro L, McAdams HH, Losick R. 2009. Why and how bacteria localize proteins. *Science* 326:1225–28
82. Stoppel R, Manavski N, Schein A, Schuster G, Teubner M, et al. 2012. RHON1 is a novel ribonucleic acid-binding protein that supports RNase E function in the *Arabidopsis* chloroplast. *Nucleic Acids Res.* 40:8593–606
83. Storz G, Vogel J, Wassarman KM. 2011. Regulation by small RNAs in bacteria: expanding frontiers. *Mol. Cell* 43:880–91
84. Strahl H, Turlan C, Khalid S, Bond PJ, Kebalo JM, et al. 2015. Membrane recognition and dynamics of the RNA degradosome. *PLOS Genet.* 11:e1004961
85. Sulthana S, Basturea GN, Deutscher MP. 2016. Elucidation of pathways of ribosomal RNA degradation: an essential role for RNase E. *RNA* 22:1163–71
86. Sulthana S, Deutscher MP. 2013. Multiple exoribonucleases catalyze maturation of the 3′ terminus of 16S ribosomal RNA (rRNA). *J. Biol. Chem.* 288:12574–79
87. Surovtsev IV, Jacobs-Wagner C. 2018. Subcellular organization: a critical feature of bacterial cell replication. *Cell* 172:1271–93
88. Tejada-Arranz A, Galtier E, El Mortaji L, Turlin E, Ershov D, De Reuse H. 2020. The RNase J-based RNA degradosome is compartmentalized in the gastric pathogen *Helicobacter pylori*. *mBio* 11(5):e01173-20
89. Tejada-Arranz A, Matos RG, Quentin Y, Bouilloux-Lafont M, Galtier E, et al. 2021. RNase R is associated in a functional complex with the RhpA DEAD-box RNA helicase in *Helicobacter pylori*. *Nucleic Acids Res.* 49:5249–64
90. Tokunaga M, Imamoto N, Sakata-Sogawa K. 2008. Highly inclined thin illumination enables clear single-molecule imaging in cells. *Nat. Methods* 5:159–61
91. Tsai YC, Du D, Dominguez-Malfavon L, Dimastrogiovanni D, Cross J, et al. 2012. Recognition of the 70S ribosome and polysome by the RNA degradosome in *Escherichia coli*. *Nucleic Acids Res.* 40:10417–31
92. Vanzo NF, Li YS, Py B, Blum E, Higgins CF, et al. 1998. Ribonuclease E organizes the protein interactions in the *Escherichia coli* RNA degradosome. *Genes Dev.* 12:2770–81
93. Vogel J, Luisi BF. 2011. Hfq and its constellation of RNA. *Nat. Rev. Microbiol.* 9:578–89
94. Voss JE, Luisi BF, Hardwick SW. 2014. Molecular recognition of RhlB and RNase D in the *Caulobacter crescentus* RNA degradosome. *Nucleic Acids Res.* 42:13294–305
95. Wang S, Moffitt JR, Dempsey GT, Xie XS, Zhuang X. 2014. Characterization and development of photoactivatable fluorescent proteins for single-molecule-based superresolution imaging. *PNAS* 111:8452–57
96. Wang X, Reyes-Lamothe R, Sherratt DJ. 2008. Visualizing genetic loci and molecular machines in living bacteria. *Biochem. Soc. Trans.* 36:749–53
97. Weng X, Bohrer CH, Bettridge K, Lagda AC, Cagliero C, et al. 2019. Spatial organization of RNA polymerase and its relationship with transcription in *Escherichia coli*. *PNAS* 116:20115–23
98. Yao Z, Carballido-López R. 2014. Fluorescence imaging for bacterial cell biology: from localization to dynamics, from ensembles to single molecules. *Annu. Rev. Microbiol.* 68:459–76
99. Young KD. 2006. The selective value of bacterial shape. *Microbiol. Mol. Biol. Rev.* 70:660–703
100. Zundel MA, Basturea GN, Deutscher MP. 2009. Initiation of ribosome degradation during starvation in *Escherichia coli*. *RNA* 15:977–83